Thermochimica Acta, 183 (1991) 125–136
Elsevier Science Publishers B.V., Amsterdam

Conventional kinetic analysis of the thermogravimetric curves for the thermal decomposition of a solid [a]

Nobuyoshi Koga and Haruhiko Tanaka

Chemistry Laboratory, Faculty of School Education, Hiroshima University, Shinonome, Minami-ku, Hiroshima, 734 (Japan)

(Received 4 September 1990)

Abstract

Kinetic obedience and Arrhenius parameters for the isothermal and non-isothermal dehydration of crushed crystals of lithium sulphate monohydrate were determined by TG using eight methods including differential and integral methods. Different apparent Arrhenius parameters were obtained by the different methods, including the differential and integral methods as well as the isothermal and non-isothermal methods. The difference in the kinetic results determined by the different methods is explained on the basis of the nature of these methods. The causation of the so-called kinetic compensation effect observed for a given dehydration reaction is discussed in connection with the reliability of TG data and the applicability of the calculation method.

INTRODUCTION

It is well known that kinetic parameters such as a kinetic rate function and the Arrhenius parameters calculated from the thermoanalytical (TA) data for the thermal decomposition of a solid vary, depending on the sample and measuring conditions [1]. In addition, although a large number of methods for kinetic analysis have been proposed for the solid state reactions [2–4], the kinetic parameters determined by different methods are also variable even under restricted experimental conditions [5]. To characterize the kinetics of a selected solid state decomposition more comprehensively, it is necessary to evaluate the reliability and significance of the respective sets of kinetic parameters, obtained by using various methods of calculation under restricted experimental conditions, as well as the effect of experimental conditions on the kinetic parameters.

[a] Part of this work was presented at the Second Japan–China Joint Symposium on Calorimetry and Thermal Analysis, 30 May–1 June 1990, Osaka, Japan.

0040-6031/91/$03.50

In this study we have examined the significance and relationship of the respective sets of kinetic parameters, determined using different methods: three and five methods for the isothermal and non-isothermal dehydration respectively, of crushed crystals of lithium sulphate monohydrate under selected experimental conditions. In addition, the cause of the variation in the kinetic parameters is discussed in connection with shortcomings inherent in the conventional thermogravimetric (TG) measurements and kinetic treatment of these data for the thermal decomposition of a solid.

EXPERIMENTAL

Single crystals of $Li_2SO_4 \cdot H_2O$ were grown from a supersaturated aqueous solution at ambient temperature. These single crystals were crushed with a pestle and mortar and sieved to a $-100 + 170$ mesh fraction. The sample was identified by TG and IR spectroscopy, and stored for about 3 weeks before measurement to avoid an ageing effect on the kinetics. Isothermal mass-loss measurements were carried out on a Shimadzu TGA-50 system in a flow of nitrogen at a rate of 30 ml min^{-1}, with 15.0 mg of sample in a platinum crucible 5 mm in diameter and 2.5 mm in height. In this system, a temperature sensor was positioned at a distance of about 1.0 mm under the crucible. The deviation of measured temperatures from those programmed was within ± 0.2°C during the course of reaction. Non-isothermal TG measurements were also made under conditions otherwise identical with those for the isothermal runs. The deviation of heating rates from those programmed was within ± 0.1 K min^{-1}.

The data obtained from mass loss measurements were processed kinetically with a microcomputer. The linearity of plots was assessed in terms of the correlation coefficient γ and/or the standard deviation σ of linear regression analyses to determine the kinetic obedience and Arrhenius parameters.

RESULTS AND DISCUSSION

Isothermal analysis

Figure 1 shows typical plots of the fractional reaction α and the rate of conversion $d\alpha/dt$ against time t for the isothermal dehydration at various constant temperatures. Longer induction periods were observed for curves measured at lower temperatures. This might be due to the reverse reaction and to the fluctuation of sample temperature, caused by the initiation of endothermic processes such as the breaking of chemical bonds and the evolution of gaseous products [2], because there is a shorter induction period

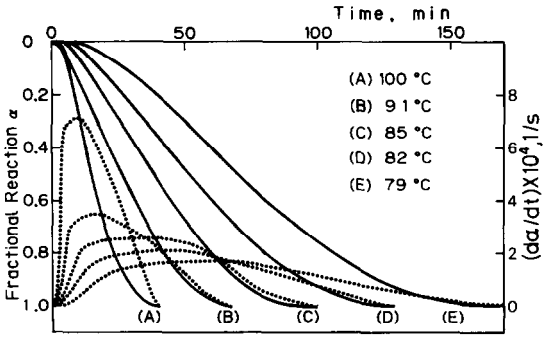

Fig. 1. Typical α vs. t (———) and $d\alpha/dt$ vs. t (···) plots for isothermal dehydration at various constant temperatures.

for the measurements with simultaneous TG–DSC [1]. The process is, as a whole, of sigmoid type, in contrast with those for the single-crystal materials in an initially evacuated constant-volume apparatus [6], where the process was predominantly deceleratory. The pattern of kinetic behaviour is more clearly illustrated by the plots of $d\alpha/dt$ against α, as shown in Fig. 2. The maximum rate is observed at smaller values of α for curves at higher temperatures. One of the reasons for the change in the α value at maximum rate, α_{max}, depending on the temperature measured, is likely to be the effect of self-cooling on the rate of dehydration; this is supported by the appearance of an induction period. Under the circumstances, it is likely that there is some distribution of the fractional conversion for each particle in a crucible owing to gradients of temperature and partial pressure of water vapour [7]. Another possibility may be a change in the diffusion rate of gaseous products relative to the rate of breaking of chemical bonds [8], i.e. the increase in the rate of breaking of chemical bonds, caused by increase in the reaction temperature, is more marked than the corresponding increase in the rate of diffusion of water vapour through the solid product layer in a

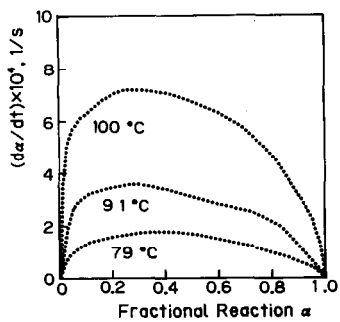

Fig. 2. Typical relationships between $d\alpha/dt$ and α for isothermal dehydration at various constant temperatures.

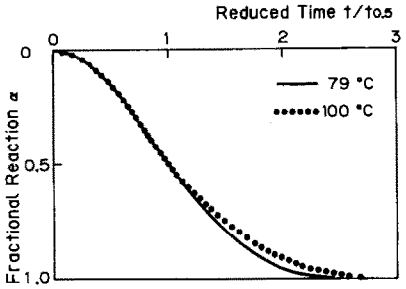

Fig. 3. Plots of α against $t/t_{0.5}$ for isothermal dehydration at 79 and 100 °C.

particle and/or the matrix. Figure 3 shows, for a rough comparison, the plots of α against $t/t_{0.5}$, where $t_{0.5}$ is the time at $\alpha = 0.5$, obtained for the isothermal mass loss traces at 79 and 100 °C. The curve for the higher temperature is delayed from that for the lower temperature as reaction advances. This trend is in qualitative agreement with the above assumption. Under such conditions, the partial pressure of the water vapour at the reaction front increases with temperature, particularly at a later stage of the reaction.

Through plots of the possible kinetic model functions, $F(\alpha)$, against t, the appropriate $F(\alpha)$ and the rate constant k were determined according to the equation

$$F(\alpha) = kt \tag{1}$$

The fairly linear plots were obtained in terms of the contracting geometry (R_n) laws, $1-(1-\alpha)^{1/n} = kt$, with $n = 2$ and 3 and the Avrami–Erofeyev (A_m) law, $[-\ln(1-\alpha)]^{1/m} = kt$, with $m = 2$ within $0.1 \leq \alpha \leq 0.9$. Figure 4 shows typical $F(\alpha)$ vs. t plots at 90 °C. The more appropriate laws were derived by scanning the values of n and m in the R_n and A_m laws respectively. Table 1 lists the values of k obtained in terms of these n and m

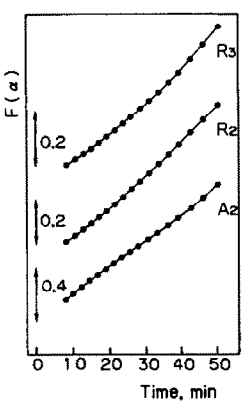

Fig. 4. Typical plots of $F(\alpha)$ vs. t for isothermal dehydration at 90 °C.

TABLE 1

The rate constant k obtained by assuming the most appropriate n and m values in the R_n and A_m laws at various constant temperatures ($0.1 \leq \alpha \leq 0.9$)

Temp. (°C)	n	$k \times 10^4$ (s^{-1})	γ [a]	σ [b] $\times 10^2$	m	$k \times 10^4$ (s)	γ [a]	σ [b] $\times 10^2$
79	1.47	1.29±0.02	0.9990	1.01	2.13	1.91±0.02	0.9997	0.89
82	1.47	1.58±0.02	0.9994	0.75	2.13	2.34±0.01	0.9998	0.65
85	1.30	2.26±0.02	0.9996	0.62	2.38	2.91±0.03	0.9995	0.93
88	1.30	2.79±0.02	0.9997	0.51	2.33	3.66±0.04	0.9994	1.05
91	1.50	2.93±0.01	0.9999	0.29	2.04	4.51±0.05	0.9993	1.23
94	1.45	3.90±0.02	0.9998	0.43	2.13	5.75±0.05	0.9995	1.03
97	1.49	4.63±0.03	0.9998	0.44	2.04	7.15±0.06	0.9996	1.00
100	1.51	5.54±0.03	0.9998	0.43	2.04	8.61±0.07	0.9996	0.97

[a] Correlation coefficient for the linear regression analysis of the $F(\alpha)$ vs. t plot.
[b] Standard deviation for the least-squares fitting of the $F(\alpha)$ vs. t plot.

values at the respective temperatures. We see from Table 1 that nearly constant values of n and m are obtained independently of the temperature measured, in contrast with the possible variation in the rate process with temperature. Although the physicochemical meaning of the non-integral values of n and m cannot be fully explained, it may be ascribed to some deviations of the measured rate processes from the theoretical reaction model. The apparent Arrhenius parameters, E and log A, determined, by assuming the mean values of n and m, from the Arrhenius equation are shown in Table 2. The E value is smaller by about 10 kJ mol^{-1} than those obtained from the measurements by simultaneous TG–DSC in a flow of N_2 [1] and under evolved gas pressure in an initially evacuated constant-volume apparatus [6]. The Arrhenius parameters are nearly equal, irrespective of the kinetic law assumed [9]. We note that it is difficult to single out the correct $F(\alpha)$ from this method, because there is a possibility that the rate process changes, depending on α, T etc. [1]. This is also because there is an overlap of analytical forms of $F(\alpha)$ for different rate-controlling processes [10].

TABLE 2

Appropriate $F(\alpha)$ and Arrhenius parameters obtained from conventional isothermal analysis within $0.1 \leq \alpha \leq 0.9$

$F(\alpha)$	E (kJ mol^{-1})	log A (s^{-1})	$-\gamma$ [a]	σ [b] $\times 10^2$
$R_{1.44 \pm 0.02}$	79.6±0.7	7.94±0.10	0.9965	4.35
$A_{2.15 \pm 0.03}$	79.5±0.7	8.10±0.10	0.9965	4.33

[a] Correlation coefficient for the linear regression analysis of the Arrhenius plot.
[b] Standard deviation for the least-squares fitting of the Arrhenius plot.

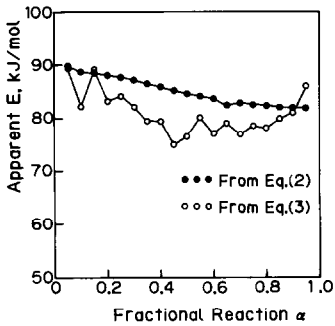

Fig. 5. Values of E at various values of α for isothermal dehydration.

The apparent activation energies, E, at various α were calculated by assuming the following integral and differential equations [11]:

$$-\ln t = -E/RT + \ln[A/F(\alpha)] \tag{2}$$

and

$$\ln(\mathrm{d}\alpha/\mathrm{d}t) = -E/RT + \ln[Af(\alpha)] \tag{3}$$

where $f(\alpha)$ is the derivative kinetic model function. The values of E at various values of α from 0.05 to 0.95 in steps of 0.05 are shown in Fig. 5. The E values obtained according to eqn. (2) decrease slightly as reaction advances. Those obtained according to eqn. (3), however, fluctuate during the course of reaction, showing the minimum value near $\alpha = 0.4$. It must be remembered, however, that the present isoconversion methods expressed by eqns. (2) and (3) are applied, in a strict sense, beyond the implicit restriction that the rate behaviour is constant irrespective of the temperature examined. At the same time, the variation in E values during the course of reaction reflects the change in rate behaviour caused by the effects of some physicochemical factors and/or of the self-generated reaction conditions. The difference in E values calculated according to eqns. (2) and (3) can be interpreted as the difference in the nature of these methods. The E values according to eqn. (2) are largely influenced by the preceding reaction process, and are less sensitive both to changes in the rate process and to experimental errors than those according to eqn. (3).

Non-isothermal analysis

Figure 6 shows the non-isothermal TG and DTG curves at various heating rates, β. From these curves, the values of E at various values of α were calculated according to the following equations proposed by Ozawa [12,13] and Friedman [14], respectively:

$$\ln(\beta/T^2) \approx -E/RT + \ln(R/\theta E) \tag{4}$$

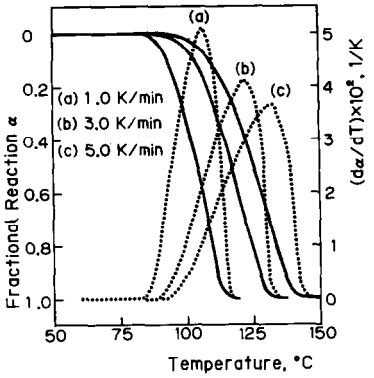

Fig. 6. Typical TG (———) and DTG (· · ·) curves for non-isothermal dehydration at various heating rates.

and

$$\ln[(\mathrm{d}\alpha/\mathrm{d}t)\beta] = -E/RT + \ln[f(\alpha)A], \tag{5}$$

where θ is the reduced time or generalized time [15]. Figure 7 shows the plots of $\ln(\beta/T^2)$ against $1/T$ at various values of α. A plot of $\ln(\beta/T_{\max}^2)$ vs. $1/T_{\max}$ using the temperature $T_{\max}$ at the maximum reaction rate is also shown in Fig. 7. This corresponds to a plot of the Kissinger method [16]. The slope is apparently different among plots obtained using the temperatures at various constant values of α and at the maximum reaction rate. We assume that the value of α at the maximum reaction rate changes, depending on β, as the maximum reaction rate was observed at $\alpha = 0.63$ and 0.74 for the runs at $\beta = 1.0$ K min^{-1} and $\beta = 5.0$ K min^{-1} respectively. Such an increase in the α value at the maximum reaction rate could be explained if the degree of participation of the nucleation processes in the early stage of the reaction increased with β [17]. Another possibility is that there is some deviation of the sample temperature from that of the surroundings during the reaction, which increases with β [18]. However, it was pointed out

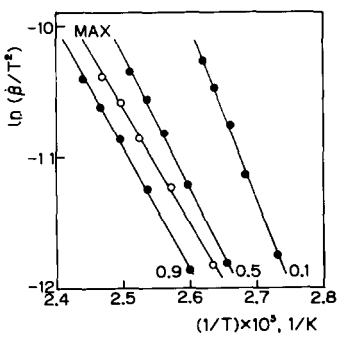

Fig. 7. Typical plots of $\ln(\beta/T^2)$ vs. $1/T$ for non-isothermal dehydration.

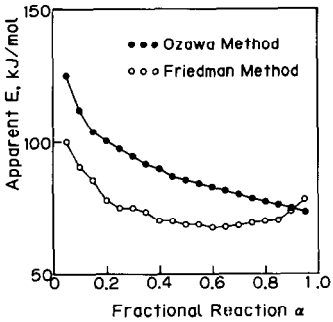

Fig. 8. The values of E at various values of α for non-isothermal dehydration.

mathematically that the α value at the maximum reaction rate changes with β [19]. As is the case with the isothermal analysis, the application of eqns. (4) and (5) is also beyond their nominal restriction. Figure 8 shows the E values at various α values obtained by the Ozawa and Friedman methods. The α dependences of the E values according to eqns. (4) and (5) show a similar trend to those obtained by isothermal isoconversion methods according to eqns. (2) and (3), respectively. Accordingly, the integral isoconversion methods, based on, for example, eqns. (2) and (4), reflect the preceding reaction processes compared with the differential isoconversion methods based on, for example, eqns. (3) and (5). It is worth noting that the E values obtained according to the differential methods are smallest around the α_{max} value. This means that these differential methods are sensitive to the self-cooling effect, which is marked around the maximum reaction rate.

The values of θ were recalculated using the mean value of E within $0.10 \leq \alpha \leq 0.90$, according to the following equation [1]:

$$\theta \approx (RT^2/\beta E) \exp(-E/RT) \tag{6}$$

In addition, the appropriate $F(\alpha)$ and pre-exponential factor A can be determined by plotting $F(\alpha)$ against θ, based on the equation [20]

$$F(\alpha) = A\theta \tag{7}$$

The fairly good linearity of the $F(\alpha)$ vs. θ plot was obtained in terms of the R_2 and A_1 laws. Table 3 lists the most appropriate $F(\alpha)$, determined by scanning the n and m values in the R_n and A_m laws, together with the

TABLE 3

Appropriate $F(\alpha)$ and Arrhenius parameters obtained from the Ozawa method for the non-isothermal reactions within $0.1 \leq \alpha \leq 0.9$

$F(\alpha)$	E (kJ mol^{-1})	A (s^{-1})	log A (s^{-1})	γ [a]
$R_{2.08}$	87.9 ± 0.8	$7.27\times10^8 \pm 1.6\times10^5$	8.86	0.9999
$A_{1.61}$	87.9 ± 0.8	$1.61\times10^9 \pm 2.2\times10^6$	9.21	0.9995

[a] Correlation coefficient for the linear regression analysis of the $F(\alpha)$ vs. θ plot.

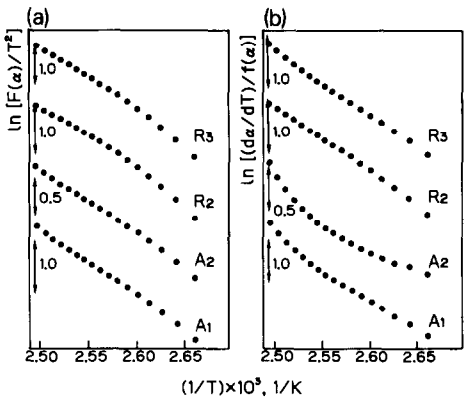

Fig. 9. Typical CR (a) and ABS (b) plots for non-isothermal dehydration at a heating rate of 3.0 K min^{-1}.

Arrhenius parameters. The E value given in Table 3 is smaller by about 25 kJ mol^{-1} and 35 kJ mol^{-1} than those determined from simultaneous measurements by TG–DSC and TG–DTA respectively [18]. It must be noted that the revised sample temperature was used in the TG–DTA analysis; this was deduced from the temperature difference between the sample and the reference material [18].

The kinetic parameters were also obtained from the TG and DTG curves at a given value β, according to the respective equations proposed by Coats and Redfern (CR) [21] and by Achar, Brindley and Sharp (ABS) [22]:

$$\ln[F(\alpha)/T^2] = \ln(AR/\beta E)[1 - 2RT/E] - E/RT \tag{8}$$

and

$$\ln[(d\alpha/dT)/f(\alpha)] = \ln(A/\beta) - E/RT \tag{9}$$

Figure 9 shows the CR and ABS plots in terms of several appropriate $F(\alpha)$ and $f(\alpha)$ functions, respectively, for the thermal dehydration at a heating rate of 3.0 K min^{-1}. Although the CR plots show good linearity in terms of the A_m laws, with $m = 1$ and 2, this is not necessarily the case with the ABS plots. This apparent anomaly is closely connected with the double logarithm in the left-hand side of eqn. (8) for the A_m laws, which markedly decreases the sensitivity of differentiation of the original functions [23]. Table 4 shows the apparent Arrhenius parameters obtained by the CR and ABS methods in terms of the R_2 law determined by the Ozawa method. We see that the values of E and log A decrease with increasing β, as is usually observed for the thermal dehydration of many inorganic salts. Moreover, the values obtained according to eqns. (8) and (9) for a run at a given value of β differ considerably beyond the errors introduced by the approximation in the right-hand side of eqn. (8) [24,25]. It seems that the difference in the apparent Arrhenius parameters results from both the smaller sensitivity of

TABLE 4

Arrhenius parameters obtained in terms of the R_2 law by the CR and ABS methods at various β within $0.1 \leq \alpha \leq 0.9$

β (K min^{-1})	CR			ABS		
	E (kJ mol^{-1})	log A (s^{-1})	$-\gamma$ [a]	E (kJ mol^{-1})	log A (s^{-1})	$-\gamma$ [b]
1.0	151±1	17.8±0.1	0.9955	104±1	13.0±0.1	0.9943
2.0	137±1	15.6±0.1	0.9930	97±1	11.9±0.1	0.9977
3.0	121±1	13.4±0.1	0.9940	91±1	11.1±0.1	0.9983
4.0	115±1	12.5±0.1	0.9948	87±1	10.5±0.1	0.9989
5.0	110±1	11.7±0.1	0.9957	85±1	10.2±0.1	0.9997

[a,b] Correlation coefficients for the linear regression analysis of the CR and ABS plots respectively.

the CR method to the rate behaviour and the error in the TG data, which is not negligible, particularly when the ABS method is used. It is noted that the Arrhenius parameters also change drastically, depending on the assumed $F(\alpha)$ and $f(\alpha)$ functions, in contrast with the results of isothermal analysis.

Reliability of TG data and significance of kinetic parameters

It is necessary here to note that the calculated Arrhenius parameters change according to the values of α and β (including the isothermal reaction when $\beta = 0$) with the so-called kinetic compensation behaviour [26]. This can be explained as a mathematical consequence of the interdependence among E, log A and the reaction temperature range ΔT which might be ascribed to the shorter temperature interval analysed [27]. Although a wider temperature interval is required for a reliable determination of the Arrhenius parameters [3], rather shorter intervals are often inevitable due to the requirement for measurements [1]. For such shorter ΔT, the apparent values of E and log A are directly influenced by the variation in ΔT due to the change in experimental conditions. Accordingly, it does not seem safe to accept the apparent Arrhenius parameters obtained from the conventional kinetic analysis of the TG curves without considering such a compensation effect.

The variation in the reaction temperature range accompanied by the change in the shape of TG and DTG curves also arises from experimental non-realization of the idealized reaction condition. One example is the deviation of sample temperature from that programmed, which is largely due to the self-cooling effect during the reaction [18]. In view of this, there are shortcomings inherent in TG and/or TG–DTA measurements similar to those for DTA, which has often been criticized as being unsuitable for kinetic use [28]. Moreover, as for TG, it is sometimes difficult to detect such

a temperature deviation, as is the case with the present TG measurements. Another factor is the change in partial pressure of the evolved gas at the reaction front during the reaction [7,8,29]. This is closely connected with the nature of the solid product layer, as well as the thickness of the layer, because any change in the rate of diffusion of the gas evolved at the reaction interfaces directly influences the partial pressure at the reaction front. In this connection, it must be borne in mind that the partial pressure inside the matrix cannot, in a strict sense, be specified in the conventional TG measurement, even if the atmosphere outside the matrix is nominally controlled and specified.

The variation in apparent kinetic parameters due to the calculation method used should be explained by the applicability of these methods to the reaction under examination and the reliability of the TG data. In spite of the difficulty in obtaining the kinetic parameters uniquely, it is desirable that the constant kinetic parameters should be obtainable, irrespective of the calculation method used, from the TG curves obtained under well-controlled conditions for the reaction in which there is no change in kinetic obedience with α, T and β examined. At the same time, the difference in the kinetic parameters due to different calculation methods may itself suggest some characteristics of the reaction kinetics or inaccuracy of the TG data. Although it is generally acceptable from the theoretical point of view that the differential methods are more suitable than integral methods in obtaining meaningful kinetic parameters [3], it is evident that success depends on the reliability of the TA data.

In discussing the kinetics of the thermal decomposition of a solid based on the kinetic parameters determined by conventional TG methods, it is important to take into account the causation of any variation in the kinetic parameters, which in turn leads to a wider comprehension of such kinetics.

ACKNOWLEDGEMENT

The authors wish to thank Dr. J. Šesták for helpful suggestions regarding the manuscript.

REFERENCES

1 N. Koga and H. Tanaka, J. Phys. Chem., 93 (1989) 7793.
2 M.E. Brown, D. Dollimore and A.K. Galwey, Reactions in the Solid State, Elsevier, Amsterdam, 1980.
3 J. Šesták, Thermophysical Properties of Solids, Elsevier, Amsterdam, 1984.
4 M.E. Brown, Introduction to Thermal Analysis, Chapman and Hall, London, 1988.
5 H. Tanaka and N. Koga, J. Phys. Chem., 92 (1988) 7023.
6 A.K. Galwey, N. Koga and H. Tanaka, J. Chem. Soc., Faraday Trans., 86 (1990) 531.
7 H. Tanaka and N. Koga, Thermochim. Acta, 173 (1990) 53.

8 N. Koga and H. Tanaka, Solid State Ionics, 44 (1990) 1.
9 H. Tanaka, S. Ohshima and H. Negita, Thermochim. Acta, 53 (1982) 161.
10 M.E. Brown and A.K. Galwey, Thermochim. Acta, 29 (1979) 129.
11 J.H. Flynn, J. Therm. Anal., 34 (1988) 367.
12 T. Ozawa, Bull. Chem. Soc. Jpn., 38 (1965) 1881.
13 T. Ozawa, J. Therm. Anal., 2 (1970) 301.
14 H.L. Friedman, J. Polym. Sci., Part C, 6 (1964) 183.
15 T. Ozawa, Thermochim. Acta, 100 (1986) 109.
16 H.E. Kissinger, Anal. Chem., 29 (1957) 1702.
17 A.A. van Dooren and B.W. Muler, Thermochim. Acta, 65 (1983) 257.
18 H. Tanaka and N. Koga, J. Therm. Anal., in press.
19 B.T. Tang and M.M. Chaushri, J. Therm. Anal., 18 (1980) 247.
20 N. Koga and H. Tanaka, J. Therm. Anal., 34 (1988) 177.
21 A.W. Coats and J.P. Redfern, Nature (London), 201 (1964) 68.
22 B.N. Achar, G.W. Brindley and J.H. Sharp, Proc. 1st Int. Clay Conf., Jerusalem, 1966, p. 67.
23 J. Šesták, J. Therm. Anal., 16 (1979) 503.
24 A.J. Kassman, Thermochim. Acta, 84 (1985) 89.
25 A. Broido and F.A. Williams, Thermochim. Acta, 6 (1973) 245.
26 N. Koga and H. Tanaka, J. Therm. Anal., in press.
27 N. Koga and J. Šesták, Thermochim. Acta, in press.
28 J. Šesták, Thermochim. Acta, 98 (1986) 339.
29 H. Tanaka and N. Koga, Thermochim. Acta, 163 (1990) 295.